

Performance Results from the First Science Run of ZEPLIN-III

Henrique Araújo

Imperial College London & STFC Rutherford Appleton Laboratory, UK

on behalf of Vadim Lebedenko[†] & ZEPLIN-III Collaboration*

[†]*In memoriam*

**Edinburgh University (UK), Imperial College London (UK), ITEP-Moscow (Russia), LIP-Coimbra (Portugal), STFC Rutherford Appleton Laboratory (UK)*

Abstract

The ZEPLIN-III experiment has just completed its first stage at the Boulby Underground Laboratory in search of dark matter WIMPs. We report on the successful operation of the instrument over the continuous 5-month run devoted to collection of WIMP search data and extensive calibration, and present preliminary performance results. Low threshold in the light and ionisation channels and excellent discrimination of γ -ray backgrounds have been achieved.

Key words: ZEPLIN-III, Dark Matter WIMPs, Two-Phase Xenon Detectors
PACS: 95.35.+d, 14.80.Ly, 29.40.Mc, 29.40.Gx

1 Introduction

ZEPLIN-III is a two-phase xenon experiment deployed 1100 m underground at the Boulby mine (UK) to search for galactic dark matter WIMPs [1,2]. It operates on the principle that electron and nuclear recoils, produced in liquid xenon (LXe) by different particle species, generate different relative amounts of scintillation light and ionisation charge. WIMPs are expected to scatter elastically off Xe atoms (much like neutrons), and the recoiling atom will produce a different signature to γ -rays, which create electron recoils. In this hybrid detector, the vacuum ultraviolet (VUV) photons generated by the scintillation (*S1*) and, indirectly, the ionisation channels (*S2*) are measured by the same array of 31 photomultiplier tubes (PMTs) immersed in the LXe.



Fig. 1. The PMT array (left), which sits at low temperature inside the LXe vessel; detector located in neutron shield at Boulby (centre); completed lead ‘castle’ (right).

We describe the instrument performance and calibration results from the First Science Run (FSR) just concluded. Overall, the detector demonstrated great stability at high electric field over several months of uninterrupted operation, and is vindicating the key aspects of our design: high-field operation (4 kV/cm in LXe) allied to surface-less 3D fiducialisation of the LXe target for excellent nuclear/electron recoil discrimination; construction using a narrow selection of low background, xenon-friendly materials proved equally important, in spite of posing considerable technical challenges. These features should be considered in the design of future systems exploiting the two-phase technique.

2 The First Science Run

By mid Feb’08 the shield had been installed around the detector, as shown in Fig. 1. It consists of 30 cm of polypropylene for moderating and absorbing neutrons from the cavern rock. Around it, 20 cm of lead (smelted and boxed) mitigate against γ -rays. This lead-hydrocarbon combination reduces both the external neutron and γ -ray fluxes by $\sim 10^5$.

After calibration runs aimed at fine-tuning the operating parameters, the FSR started on 27 Feb’08. Over the following 84 days we recorded high-quality WIMP-search data with an 84% duty-cycle; the remaining few hours were devoted to a daily calibration with ^{57}Co γ -rays, topping up the detector with LN_2 and general data management, including extraction of a 10% data sample for dip-test analysis and calculation of electron-recoil backgrounds. Overall, some 27 TB of data (uncompressed) were recorded during the ‘dark’ run, and a similar amount during the ensuing calibration stage. An exposure of 450 kg \times days was collected for the 6.5 kg fiducial mass inside 150 mm reconstructed radius and a liquid height of 32 mm.

The low-energy electron-recoil background, shown in Fig. 2 (left), is measured at 14.0 ± 0.5 dru (1 dru = 1 evt/kg/day/keVee, where ‘ee’ stands for ‘electron equivalent’), in good agreement with our predictions for the PMT array

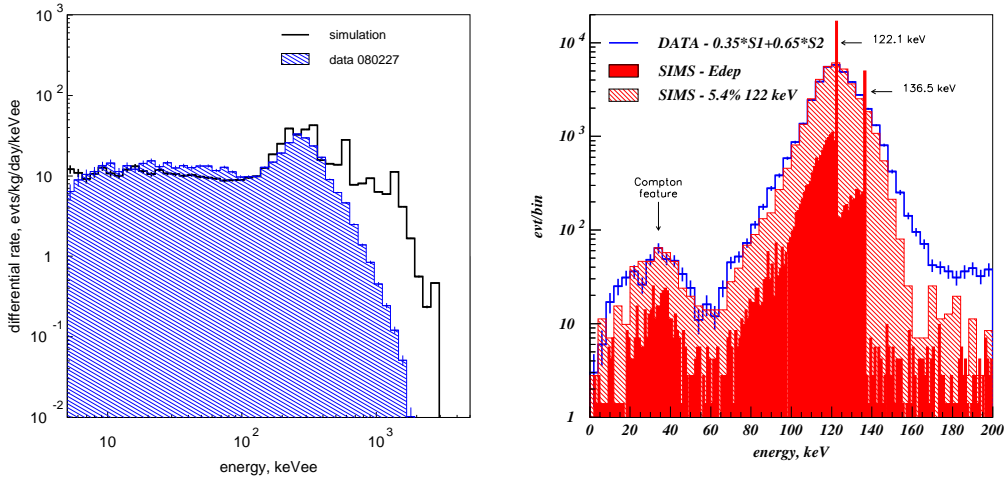


Fig. 2. Left: Electron-recoil background in the ‘dark’ run, in agreement with our prediction at low energies. Right: ^{57}Co calibration compared to simulation results; the latter are smeared by an energy resolution $\sigma = 0.60\sqrt{E}$ [keV].

(10.5 dru), γ -rays from the Pb castle (0.7 dru), feedthroughs (0.1 dru) and ^{85}Kr β s (0.2 dru); systematic errors in the simulation are comparable to the observed discrepancy. The disagreement at high energies is caused by single-scatter selection in the data (but not in the simulation) and by DAQ saturation. This result reinforces our prediction of ~ 1 neutron event expected for the FSR data-set, and justifies our decision to upgrade the PMTs in phase II.

The ^{57}Co runs provided energy calibration of the $S1$ and $S2$ responses and monitoring of their stability. These data also serve for routine measurement of the electron lifetime, detector tilt, liquid level and pressure effects – variables that affect mainly the electroluminescence signal. Only the electron lifetime was corrected for in the science data (the other effects play a role at the percent level). A lifetime of 20 μs was achieved at the beginning of the run through getter purification, which is sufficient for our needs since the full-length drift time in the chamber is only 14 μs . Unexpectedly, the measured lifetime *increased* steadily, reaching ~ 35 μs by the end of the run, which we attribute to steady migration of electronegative impurities (or their negative ions) under the electric field, which remained undisturbed throughout. We note that the observed electron capture cross-section exhibits a strong field dependence, showing a ten-fold increase at our operating field.

The energy spectrum from one day’s ^{57}Co data is shown in Fig. 2 (right), derived from a linear combination of $S1$ and $S2$ in order to exploit the anti-correlation of these channels – whereby an ionisation electron can *either* contribute to the $S2$ charge signal *or* to the light signal (through recombination). We obtain an energy resolution $\sigma=5.4\%$ at 122 keV, compared to 16.3% for $S1$ and 8.8% for $S2$ alone. A preliminary analysis indicates a light yield of 1.8 phe/keVee at nominal field, reduced from 5.0 phe/keVee at zero field.

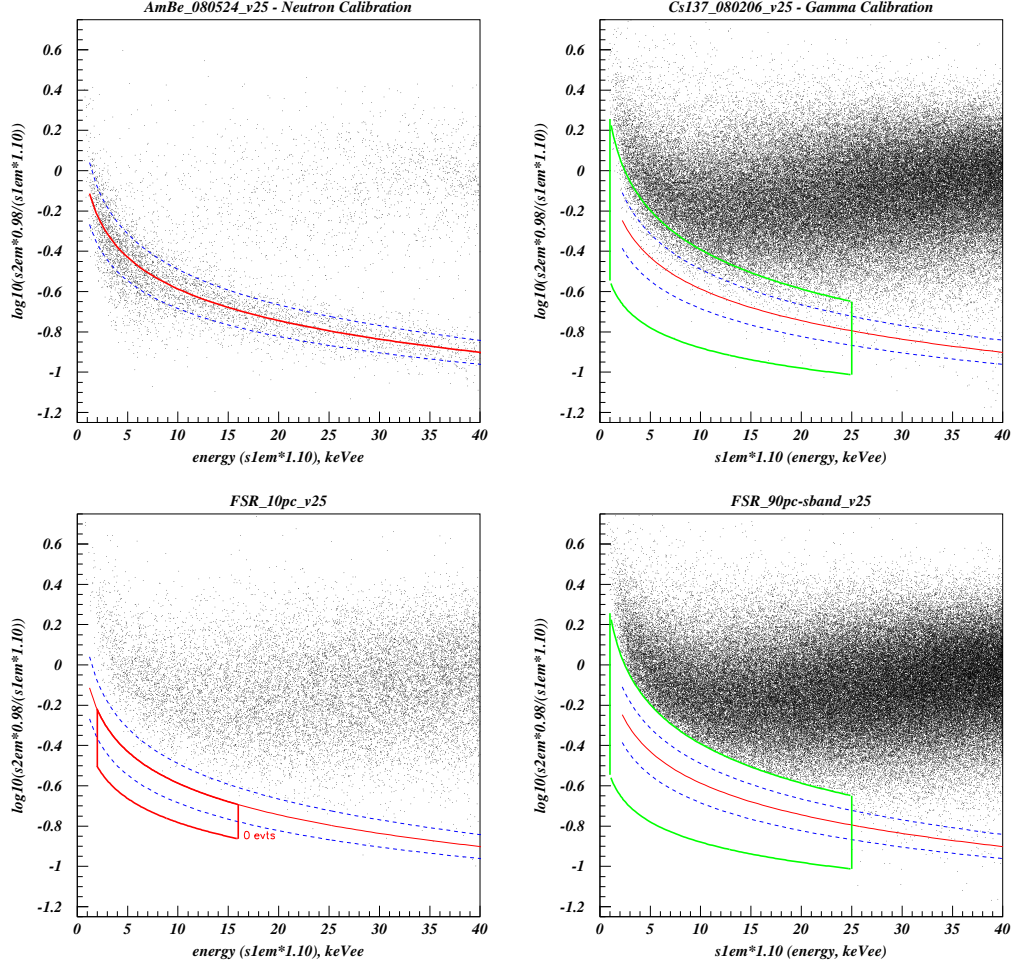


Fig. 3. a) Am-Be neutron calibration, showing mean and $\pm\sigma$ lines from Gaussian fits to $\log(S_2/S_1)$; b) ^{137}Cs calibration, showing region earmarked for sideband analysis of the FSR data-set; c) 10% ‘dark’ data sample with no events in the chosen WIMP acceptance region; d) main FSR data-set, blinded in region mentioned in b).

3 Calibration of nuclear- and electron-recoil responses

The 84-day ‘dark’ run was followed by extensive calibration with Am-Be neutrons (5 hours) to calibrate the response to elastic recoils, and with ^{137}Cs γ -rays (122 hours) to populate the low-energy electron-recoil region through Compton scattering. The ^{137}Cs data-set is approximately equivalent to the ‘dark’ exposure in number of low-energy events.

The neutron data-set is summarised in Fig. 3 a), showing the discrimination parameter (essentially the ratio S_2/S_1 for calibrated pulse areas) as a function of electron-equivalent energy derived from S_1 . The conversion to nuclear recoil energy considered here is $\text{keVnr}=2.09 \text{ keVee}$, which assumes a constant 19% relative scintillation efficiency for nuclear recoils relative to ^{57}Co γ -rays at

zero field, 64% field-induced suppression of scintillation for electrons and 10% for nuclear recoils. We are presently investigating how well these assumptions hold for the energy range of interest. The trend of the means and standard deviations of log-normal fits over narrow energy bins is also shown for the elastic population. Excellent energy thresholds were achieved for elastic recoil detection: ≈ 1.5 keVee in the S1 channel (software threshold) and < 1 keVee in the S2 channel (hardware trigger).

The Compton calibration, carried out at a low rate of tens of c/s, shows excellent agreement with the science data at first inspection. However, there is a subtle difference in the behaviour of the γ -ray distribution well below the mean, especially at higher energies: consistently more events are seen in the calibration than in the unveiled sidebands of the ‘dark’ data-set, as shown in Fig. 3 b) and d). This is due to an important population of relatively rare double-scatter events, which we know colloquially as ‘living-dead’ since they scatter once in the active (live) region and once in a dead region with no charge extraction (such as under the cathode grid located just above the PMTs). The fact that the ^{137}Cs data fail to reproduce this population accurately is not surprising, since this event topology is very sensitive to the directionality of the γ -ray flux: the ^{137}Cs source was located above the detector whereas most of the background originates in the PMTs underneath the fiducial volume. For this reason, the ^{137}Cs data-set is of limited value in helping to predict the leakage of this population into the nuclear recoil acceptance region. In spite of this, the γ -ray discrimination achieved is the highest reported for any two-phase xenon experiment: we estimate that fewer than $\sim 2 \cdot 10^4$ electron recoil events leaks below the nuclear recoil median line near threshold.

Using calibration data and the 10% sample, a WIMP acceptance region has been defined in the energy range 2-16 keVee, retaining 47.7% acceptance in the $\log(S2/S1)$ parameter (extending down by 2σ from the median line). This is shown in Fig. 3 c). We are presently working on improving our prediction of how many γ -ray events (including ‘living-dead’) are expected there in the main ‘dark’ data-set, in addition to the ~ 1 neutron event predicted by our background calculations (largely dominated by PMT neutrons). We are also improving our position reconstruction algorithms in order to increase the rejection of these ‘living-dead’ events even further.

Considering the exposure accumulated in the FSR, all efficiency factors obscuring the WIMP response (trigger efficiency, live-time fraction, pulse-finding efficiency, software cuts, nuclear recoil acceptance, etc.), together with neutron and γ -ray background predictions for that region, we are confident of at least reaching the sensitivity predicted previously [2] and of improving significantly on our result from the ZEPLIN-II experiment [3,4].

4 The next phase

Several planned upgrades are now underway in phase II of the experiment. Having confirmed that the background is dominated by the photomultipliers, we are replacing them with pin-by-pin compatible ones developed in collaboration with the manufacturer. Components for the new PMTs have been individually radio-assayed and their effect simulated. We are confident that the γ -ray and neutron backgrounds can be improved by a factor of ~ 30 .

An active scintillator veto to encompass the detector inside the lead castle is in the final stages of construction. It consists of plastic scintillator modules around and above the target. Inside this assembly, Gd-loaded hydrocarbon captures neutrons with high efficiency, producing γ -rays which can be detected by the surrounding scintillator. Tagging of 75% for neutrons inside the shield is our realistic aim. This veto also serves an important diagnostic purpose, as we probe into even rarer processes.

Although there are no outstanding issues relating to the electron lifetime, we are installing a pump-driven gas recirculation system to speed up the initial purification and to recover promptly from accidental contamination. Additional work is underway to automate the delivery of the calibration sources and of the LN₂ filling of the detector. A new, extended science run is expected to start towards the end of 2008, with improvements in operational effort, reliability and WIMP sensitivity.

5 Acknowledgements

We wish to pay tribute to our colleague and friend Vadim N. Lebedenko (1939-2008), who had a key role in designing and building this instrument. He also pioneered the two-phase detection technique with noble liquids [5].

References

- [1] D.Yu.Akimov *et al.*, *Astroparticle Phys.* **27** 46–60 (2007)
- [2] H.M.Araújo *et al.*, *Astroparticle Phys.* **26** 140–153 (2006)
- [3] G.J.Alnér *et al.*, *Astroparticle Phys.* **28** 298–302 (2007)
- [4] G.J.Alnér *et al.*, *Phys. Lett B.* **653** 161–166 (2007)
- [5] B.A.Dolgoshein, V.N.Lebedenko & B.U.Rodionov, *JETP Lett.* **11** 513 (1970)